Dynamics of dual film formation in boundary lubrication of steels
Part III. Real time monitoring with ellipsometry

Bülent Çavdar and **Kenneth C. Ludema***
Mechanical Engineering Department, University of Michigan, Ann Arbor, MI 48109-2125 (U.S.A.)

(Received October 3, 1990; revised January 21, 1991; accepted February 13, 1991)

Abstract

Effective "breaking-in" of lubricated steel surfaces has been found to be due primarily to the rate of growth of "protective" films of oxides and compounds derived from the lubricant. The protection afforded by the films is strongly dependent on lubricant chemistry, steel composition, original surface roughness and the load/speed sequence or history in the early stages of sliding. Given the great number of variables involved it is not possible to follow more than a few of the chemical changes on surfaces using the electron, ion and X-ray column analytical instruments at the end of experiments. Ellipsometry was therefore used to monitor the formation and loss of dual protective films in real time, and detailed chemical analysis was done at various stages to calibrate the ellipsometer. This work is reported in three interlinking parts: I, functional nature and mechanical properties; II, chemical analyses; III, real-time monitoring with ellipsometry.

1. Introduction

Many phenomenological studies had been done, mostly by chemists on the chemical compositions required in oil for successful functioning as a lubricant at high severities of sliding. It had been generally agreed that a "protective" film forms on well functioning sliding surfaces, but the composition and structure of the adsorbed substances remained obscure. There were two reasons for this uncertainty. Firstly, only a small amount of material was gathered from the films for analysis by some instruments (IR, X-ray diffraction). Secondly, for those analytical instruments that use the electron, ion or X-ray column, samples must be rigorously cleaned, which removes much of the interesting material. Ellipsometry does not have this limitation.

The chemical analysis of surface films is of great interest in studies of boundary lubrication. However, the major problem in the use of analytical instruments is that the act of removing the specimens from the tests for analysis produces changes in the films that are different from the changes that occur during continued sliding. Thus a method was required to monitor some aspects of chemical changes in the films *during sliding*. Realistic sliding tests cannot be done in the (vacuum) environment of the analytical instruments. Ellipsometry was chosen for real time, real environment monitoring of the sliding surfaces. The analytical instruments were used to "calibrate" the ellipsometer.

*Author to whom correspondence should be addressed.

0043-1648/91/$3.50

Conventional ellipsometry could not be used because the sliding surfaces are rough, and because the films formed during sliding are composed of several, or a gradation of, compositions from the metal surface outwards. Thus complete (four Stokes parameter) ellipsometry was used in an automated instrument for real time measurements.

The application of ellipsometry in tribology has so far been limited to "off-line" analysis, that is a specimen is removed from the friction machine and cleaned of liquids before measurement [1–3]. On-line analysis of lubricated sliding surfaces was delayed by the non-ideal effects from liquid lubricant and surface roughness which cannot be accommodated in conventional ellipsometry. Recently, some theoretical studies [4–7] focused on the effect of the surface roughness, and some optical models [8, 9] were proposed. However, as shown by Ramsey [10], no published optical model truly represents the surface roughness for ellipsometry.

In this study, ellipsometry is used in an on-line analysis of the lubricated sliding of steel surfaces. Some computational considerations and effects of the lubricant and surface roughness are discussed.

2. Polarized light

Light waves can be described as sinusoidal variations in the magnitude of an electric field E propagating in the z direction. The electric field vector can be resolved into orthogonal components E_p and E_s in the p and s direction as shown in Fig. 1. Their magnitudes vary harmonically, and can be represented by [11]:

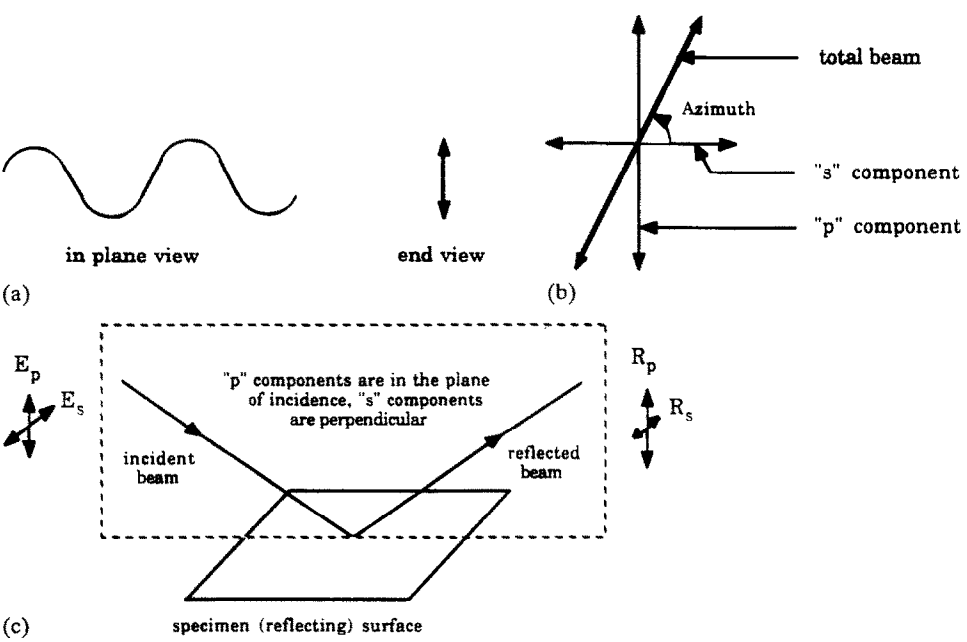

Fig. 1. Graphical representation of plane polarized light and its p and s components, shown relative to the plane of incidence: (a) linearly polarized light; (b) s and p components of a linearly polarized beam; (c) plane of incidence of light relative to the s and p components.

$$E_p = E_p \cos(\tau + \delta_p) \qquad E_s = E_s \cos(\tau + \delta_s) \tag{1}$$

where $\tau = (2\pi z/\lambda) - \omega t$, the wave propagation term, and λ and ω are the wavelength and frequency of the light wave, and $(\delta_s - \delta_p) = \delta$, is the phase difference.

If E_p and E_s are either in phase, or 180° out of phase, the resultant vector traces a planar path through space, which is called linear polarization. If, on the other hand, the relative phase of the components is either $+90°$ or $-90°$, and amplitudes E_p and E_s are equal, the tip of the E vector traces a circle with time, and is called circular polarization. In the most general case of different amplitudes E_p and E_s, coupled with an arbitrary phase difference δ, the tip of the vector will trace the pattern of an ellipse.

A light beam directed onto a surface is referred to as an incident beam. Reflected light can be treated in the same way as the incident light. An E_p component of light that is incident to the surface at an angle ϕ_1 will reflect as linearly polarized light which is called R_p. In general, there will be a change in both phase and amplitude of light upon reflection. The E_s component will have a separate but similar effect.

The relationship between the incident (i) and reflected (r) waves is defined by "reflection coefficients". Since relative amplitude and phase information must be expressed, a complex number representation is a convenient form for a reflection coefficient. Thus, reflection coefficients for p or s polarization can be written as:

$$r_p = R_p/E_p \exp\{j[(\delta_p)_r - (\delta_p)_i]\} \tag{2}$$

$$r_s = R_s/E_s \exp\{j[(\delta_s)_r - (\delta_s)_i]\} \tag{3}$$

The absolute phase difference between corresponding incident and reflected components is not a readily measurable quantity, but it is possible to determine the ratio of reflection coefficients. This ratio is:

$$\rho = \frac{R_p/R_s \exp\{j[(\delta_p)_r - (\delta_s)_r]\}}{E_p/E_s \exp\{j[(\delta_p)_r - (\delta_s)_i]\}} \tag{4}$$

If

$$\frac{R_p/R_s}{E_p/E_s} = \tan \psi$$

and

$$[(\delta_p)_r - (\delta_s)_r] - [(\delta_p)_i - (\delta_s)_i] = \Delta \tag{5}$$

then

$$\rho = \tan \psi \exp(j\Delta) \tag{6}$$

This is the fundamental equation of ellipsometry. ψ and Δ are differential changes in amplitude and phase respectively. They can be measured by conventional ellipsometry.

One type of conventional null ellipsometer consists of a light source, a polarizer, a compensator for the reflecting specimen surface and a an analyzer, which is essentially also a polarizer. The compensator is usually a quarter-wave plate which can be placed between the polarizer and specimen (or specimen and analyzer). Measurement is done by adjusting the azimuth angles of two of the three optical components, *i.e.* the polarizer, compensator and analyzer, and keeping the third component at a fixed angle so that no light passes through the analyzer. In the fixed polarizer case, a plane polarized light with its vibration direction inclined at 45° to the plane of incidence is

usually used. The reflected light is generally elliptically polarized and, since the amplitudes of the two incident components are equal (where the azimuth of the polarizer is 45°), the differential amplitude change is given by $\tan \psi = R_p/R_s$. If a phase difference equal and opposite to that occurring at the surface is introduced by the compensator, plane polarized light emerges upon reflection from the specimen surface and can be extinguished by the analyzer. The analyzer setting thus yields ψ and the compensator setting Δ. In the fixed compensator case the compensator is usually set at a fixed azimuth of $+45°$ or $-45°$. Then, the light is extinguished by alternately adjusting the polarizer and the analyzer. The analyzer setting yields ψ and the polarizer setting Δ.

It should be noted that since the operation of null ellipsometry is based on extinguishing the reflected light no attempt is made in the above to include the amplitude of light, or size of the ellipse, only the form. Stokes developed four parameters whereby the total state of polarization, including amplitude for monochromatic light, may be expressed:

$$S_0 = E_p^2 + E_s^2$$

$$S_1 = E_p^2 - E_s^2$$

$$S_2 = 2E_p E_s \cos(\delta_s - \delta_p)$$

$$S_3 = 2E_p E_s \sin(\delta_s - \delta_p) \tag{7}$$

The amplitude is included in these equations, and these four parameters may be loosely connected with four attributes of elliptically polarized light:

(1) the size of the ellipse (or the total amplitude $A = (E_p^2 + E_s^2)^{1/2}$;

(2) the ratio of minor axis length to major axis length E_p/E_s;

(3) the orientation or tilt of the major axis relative to the s direction, azimuth θ;

(4) the direction of rotation of the E vector, right-hand or clockwise rotation is defined as positive.

For completely polarized light:

$$S_0^2 = S_1^2 + S_2^2 + S_3^2 \tag{8}$$

and for incompletely polarized light:

$$S_0^2 > S_1^2 + S_2^2 + S_3^2 \tag{9}$$

The Stokes equations provide a convenient comparison between historical ellipsometry and modern ellipsometry. A major difficulty in early ellipsometry was the unavailability of stable light sources and photometers. Thus it was convenient to ignore amplitude, and coincidentally the ellipsometers that were developed on this omission required less tedious calculations. Unfortunately, a major limitation of older ellipsometers is that it is not possible to determine from the results whether non-ideal effects of the reflecting surface exist such as depolarization, cross polarization and change in ellipticity. Depolarization and other effects are common with non-homogeneous reflecting substances and with rough surfaces [11].

3. Mueller matrix ellipsometry

With the advent of computers it is possible to speed up calculations considerably, and also to take data so quickly that drift in the light source and the light sensors

have small effects. A new computerized ellipsometer was constructed in our laboratory and its principle of operation is conveniently described in terms of the Stokes parameters [12].

The four Stokes parameters can be conveniently grouped as a vector quantity S, where they are arranged as:

$$S = [S_0, S_1, S_2, S_3] \tag{10}$$

We can define one Stokes' vector for the incident light as S_I, and another vector for reflected light S_R. For any linear optical system, these two vector quantities may be related by a simple 4×4 matrix, as

$$\mathbf{S_R} = \mathbf{M}\mathbf{S_I} \tag{11}$$

This equation is an example of the Mueller calculus and **M** is a 16-element transformation matrix.

For an ideal reflective system a Mueller matrix can be derived in terms of the ellipsometric parameters Δ and ψ:

$$\mathbf{M} = \frac{r_p^2 + r_s^2}{2} \begin{bmatrix} 1 & -\cos 2\psi & 0 & 0 \\ -\cos 2\psi & 1 & 0 & 0 \\ 0 & 0 & \sin 2\psi \cos \Delta & \sin 2\psi \sin \Delta \\ 0 & 0 & -\sin 2\psi \sin \Delta & \sin 2\psi \cos \Delta \end{bmatrix} \tag{12}$$

where r_p and r_s are scalar amplitude reflection coefficients.

The new ellipsometer is capable of accommodating some unpolarized component in the light. The basic optics scheme was outlined in detail by Hauge [13] and is illustrated in Fig. 2 of Part I [14]. It consists of a tunable laser which directs light through a fixed polarizer and a rotating compensator, onto the specimen. With each rotation of the compensator, every possible state of polarized light is directed to the specimen. Reflected light passes through a second compensator, through another fixed polarizer (analyzer) and into a light-detecting diode. The second compensator rotates exactly five times as fast as the first compensator, which rotates at about 1 rev s^{-1}. The light-detecting diode receives a time-varying intensity of radiation, which function is operated upon by a Fourier transform, producing 25 coefficients. These coefficients, together with information on the wavelength of light, the instantaneous angular positions of the two polarizers and the two compensators, and the angle of incidence are used to provide the 16-element Mueller matrix.

For mildly non-ideal surfaces the matrix is not exactly symmetric (in absolute values) about the diagonal and for such cases the values of Δ and ψ may be calculated as follows;

$$\psi = 0.5 \cos^{-1} [(-M(0,1) - M(1,0))/2] \tag{13a}$$

$$\Delta = \tan^{-1} [(M(2,3) - M(3,2))/(M(2,2) - M(3,3)] \tag{13b}$$

The Mueller matrix representation of the surfaces also allows one to identify some of the non-ideal effects produced by surfaces by analyzing the asymmetry of the matrix. Williams [11] defined several parameters using the Mueller matrix formulation in order to quantify the non-ideal effects due to surface irregularities such as depolarization, cross-polarization and change in ellipticity of initially totally polarized light. The degree of non-ideal effects in our data will be discussed in this paper.

4. Calculation of substrate and film parameters with ideal interfaces

Now let us consider an ambient–substrate system (no film) as in Fig. 2(a). By assuming that the interface between the ambient and substrate is mathematically sharp and smooth, and by applying appropriate boundary conditions to the solutions of Maxwell's equations, the reflection coefficients can be written in the following form [15] (subscript 1 refers to the "medium" above the reflecting surface, subscript 2 refers to a film and subscript 3 refers to the solid substrate):

$$r_p = \frac{n_1 \cos \phi_3 - n_3 \cos \phi_1}{n_1 \cos \phi_3 + n_3 \cos \phi_1} \quad r_s = \frac{n_1 \cos \phi_1 - n_3 \cos \phi_3}{n_1 \cos \phi_1 + n_3 \cos \phi_2} \tag{14}$$

These forms of r_p and r_s are referred to as the Fresnel reflection coefficients. The corresponding Snell's law is:

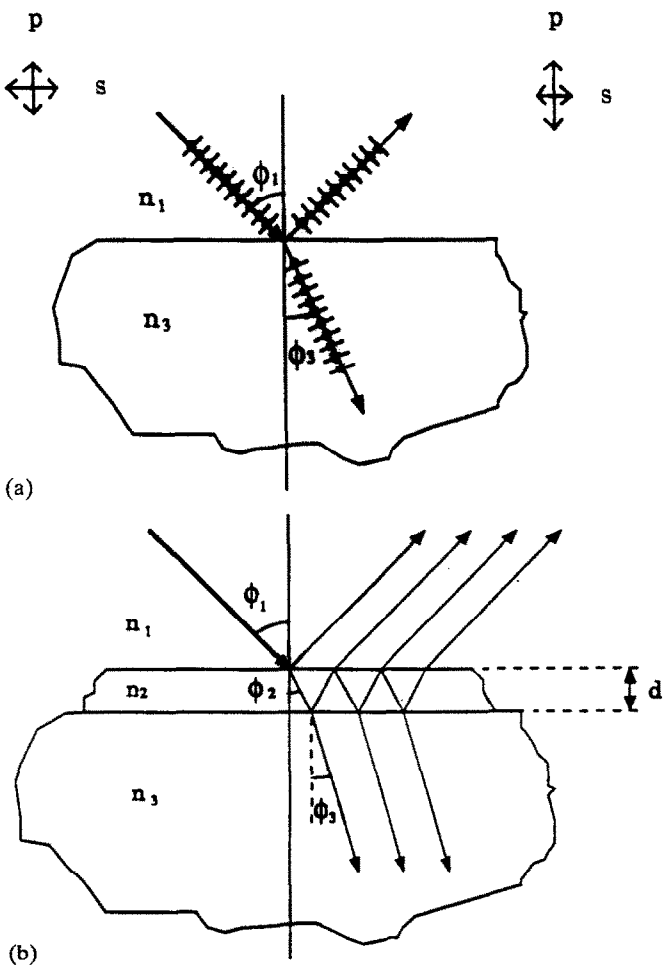

Fig. 2. The reflection, refraction and transmission of an incident light beam: (a) an ambient(1)–substrate(3) system, and (b) an ambient(1)–film(2)–substrate(3) system.

$$\frac{\sin \phi_1}{\sin \phi_3} = \frac{n_3}{n_1} \tag{15}$$

From the measured values of Δ and ψ, and using eqns. (4), (6), (14) and (15), the complex index of the substrate can be calculated by:

$$n_3 = n_1 \tan \phi_1 \left[1 - \frac{4\rho \sin^2 \phi_1}{(\rho+1)^2} \right]^{1/2} \tag{16}$$

For an ambient–*film*–substrate system (Fig. 2(b)), the multiple reflections of light within the film must be considered. The Fresnel reflection coefficients for the ambient–film interface are:

$$r_{12p} = \frac{n_1 \cos \phi_2 - n_2 \cos \phi_1}{n_1 \cos \phi_2 + n_2 \cos \phi_1} \quad r_{12s} = \frac{n_1 \cos \phi_1 - n_2 \cos \phi_2}{n_1 \cos \phi_1 + n_2 \cos \phi_2} \tag{17}$$

and the corresponding Snell's law:

$$\frac{\sin \phi_1}{\sin \phi_2} = \frac{n_2}{n_1} \tag{18}$$

Finally, the Fresnel reflection coefficients for the film–substrate interface are:

$$r_{23p} = \frac{n_2 \cos \phi_3 - n_3 \cos \phi_2}{n_2 \cos \phi_3 + n_3 \cos \phi_2} \quad r_{23s} = \frac{n_2 \cos \phi_2 - n_3 \cos \phi_3}{n_2 \cos \phi_2 + n_3 \cos \phi_3} \tag{19}$$

and the corresponding Snell's law:

$$\frac{\sin \phi_2}{\sin \phi_3} = \frac{n_3}{n_2} \tag{20}$$

As in Fig. 2(b), the light will undergo multiple reflections and upon each reflection at the ambient–film interface a fraction of light will be transmitted and a fraction will be reflected. Likewise, at the film–substrate interface a fraction will be transmitted and a fraction reflected.

The phase and amplitude of the total reflected beam emerging from the specimen are given by the Drude equations:

$$r_p = \frac{r_{12p} + r_{23p} \exp(-jD)}{1 + r_{12p} r_{23p} \exp(-jD)} \quad r_s = \frac{r_{12s} + r_{23s} \exp(-jD)}{1 + r_{12s} r_{23s} \exp(-jD)} \tag{21}$$

where D is the phase lag of the light due to the film:

$$D = (4\pi/\lambda) n_2 d \cos \phi_2 \tag{22}$$

where λ is the wavelength of the light. Hence, the fundamental equation of ellipsometry is again:

$$\rho = \frac{r_p}{r_s} = \tan \psi \exp(j\Delta) \tag{23}$$

The refractive index of the substrate, $n_3 - jk_3$, can be found from eqn. (16) by taking an ellipsometric measurement on the bare substrate. The parameters of a non-absorbing film, *i.e.* n_2 and d, can be calculated by replacing Δ and ψ values measured on the film-covered surface and using eqns. (17)–(23). Since ρ is a complex number, eqn. (23) gives two equations: one for the real part and the other for the imaginary

part. If the film is absorbing, *i.e.* if the refractive index of film is in the form $n_2 - jk_2$, in order to calculate three unknowns, n_2, k_2 and d, additional ellipsometric measurements must be made. This can be done by taking measurements at different angles of incidence and/or different wavelengths of light which usually produces more equations than the number of unknowns. A least squares fitting procedure must be used to resolve the overdetermined system of equations as described in the paragraph on data analysis below.

5. Calculation of film parameters in an oil medium (non-ideal interface)

In our study, mineral oils were used as lubricants in friction tests. The oil medium added some difficulties in the calculation of the film parameters n_2, k_2 and d because hydrocarbon molecules of oil orient themselves towards the steel surface at the oil–steel interface. For the calculations of thickness and optical constants of the films in an ideal case, one only needs to replace the refractive index of the oil medium in the above equations. However, the refractive index of oil, which can be measured by reflection from the surface of a bulk oil, does not represent the real refractive index of oil at the oil–specimen interface and therefore does not give accurate results.

Therefore, we have followed a different approach, and delay the introduction of the refractive index of oil into the equations until these properties can be measured from the operating oil–specimen interface after the experiment has been done. The mathematical sequence we use is as follows.

The Fresnel reflection coefficients are rewritten in the following form:

$$r_{12p} = \frac{\cos\phi_2 - n_{2m}\cos\phi_1}{\cos\phi_2 + n_{2m}\cos\phi_1} \qquad r_{12s} = \frac{\cos\phi_1 - n_{2m}\cos\phi_2}{\cos\phi_1 + n_{2m}\cos\phi_2}$$

$$r_{23p} = \frac{n_{2m}\cos\phi_3 - n_{3m}\cos\phi_2}{n_{2m}\cos\phi_3 + n_{3m}\cos\phi_2} \qquad r_{23s} = \frac{n_{2m}\cos\phi_2 - n_{3m}\cos\phi_3}{n_{2m}\cos\phi_2 + n_{3m}\cos\phi_3} \tag{24}$$

where

$$n_{2m} = n_2/n_1 \qquad n_{3m} = n_3/n_1 \tag{25}$$

In other words we treat the equations, at first, as if the medium were air (*i.e.* $n_1 = 1$). If we rewrite D in the same form:

$$D = (4\pi/\lambda) n_{2m} d_m \cos\phi_2 \tag{26}$$

where

$$d_m = n_1 d \tag{27}$$

and substituting eqns. (24) and (26) into eqn. (1) and then using eqn. (23), we can calculate n_{2m}, k_{2m} and d_m which we call apparent parameters. The apparent refractive index of the substrate, $n_{3m} - jk_{3m}$, can be found by taking a separate ellipsometric measurement on the bare substrate in oil and rewriting eqn. (16) in the following form:

$$n_{3m} = \frac{n_3}{n_1} = \tan\phi_1 \left[1 - \frac{4\rho\sin^2\phi_1}{(\rho+1)^2}\right]^{1/2} \tag{28}$$

When the refractive index of oil at the oil–steel interface n_1 is known, the apparent parameters n_{2m}, k_{2m} and d_m can be converted to the true values of n_2, k_2 and d using

eqns. (25) and (27). The refractive index of oil at the oil–steel interface can be found as follows. First n_3 and n_{3m} are found from eqns. (16) and (28) by taking two ellipsometric measurements respectively, one in air ($n_1 = n_{air} = 1$) and one in oil on a bare substrate. Then, $n_1 = n_{oil}$ is obtained from n_3/n_{3m} using eqn. (28). An example of application on steel gave the following results: optical constants of steel in air $n_3 - jk_3 = 2.67 - j3.44$; the apparent parameters for steel in oil $n_{3m} - jk_{3m} = 2.05 - j2.34$; thus the optical constants of oil at the oil–steel interface $n_1 - jk_1 = 1.40 - j0.08$. The refractive index of oil from the surface of a bulk oil was found to be $1.45 - j0.002$. As we see, the optical constant of oil at the oil–steel interface is different from that at the air–oil interface.

6. Sensitivity and error analysis

In order to gain a perspective on the accuracy of results a sensitivity and error analysis was done. The sensitivity of Δ and ψ values to changes in various parameters can be analytically or numerically analyzed [16, 17]. Δ and ψ values are computed for the range of angle of incidences from 1° to 90° for given values of substrate and film parameters (n_3, k_3, n_2, k_2 and d) using eqns. (14)–(23). Then, the value of one of the parameters was slightly changed and Δ and ψ values computed again for the same range of ϕ. The difference between the first set of Δ and ψ values and the second set gives the sensitivity of ellipsometric parameters to that slight change. The sensitivities are plotted as a function of angle of incidence. Two such sensitivity curves for Δ and ψ are shown in Fig. 3.

It is seen from Fig. 3(a) that the highest sensitivities of Δ and ψ values to an increase of 1 Å in the thickness of a 100 Å thick oxide film on a steel substrate are obtained at angles between 65° and 80°. Figure 3(b) shows the sensitivities of Δ and ψ values to the 0.01° error in the determination of the angle of incidence. By comparing Figs. 3(a) and (b), it is seen that the sensitivities of Δ and ψ values to a 1 Å increase in the film thickness is about four times higher than their sensitivities to a 0.01° error in the determination of the angle of incidence. In our ellipsometer, the angles of the polarizer and analyzer arms were set by stepping motors automatically with an accuracy of $\pm 0.005°$. The error in Δ and ψ coming from the inaccuracies of the angle of incidence is therefore negligible. As is shown in Fig. 3(b), Δ and ψ become more sensitive to errors in the angle of incidence for higher angles of incidence than 75°; therefore, the use of angles of incidence greater than 75° should be avoided.

The standard random error in the determination of ψ was 0.02° and that of Δ was 0.2°. As seen from Fig. 3(a), this much error in Δ and ψ values leads to an uncertainty of only ± 1 Å in the calculations of film thickness.

7. Data analysis

As mentioned before, when there are more than two unknown parameters to be determined, the problem is a little more complicated. Additional equations can be provided by making measurements at multiple angles of incidence. In this case the number of equations usually exceeds the number of unknowns. Hence, the problem of the overdetermined system of equations occurs.

A non-linear least squares fitting procedure (Marquardt method [18]) is used to calculate n, k and d of films by minimizing an error function G in the form of:

$$G(\boldsymbol{B}) = \sum_{i=1}^{m} \{[\Delta_i^m - \Delta_i^c(\boldsymbol{B}, \phi_i)]^2 + [\psi_i^m - \psi_i^c(\boldsymbol{B}, \phi_i)]^2\} \tag{29}$$

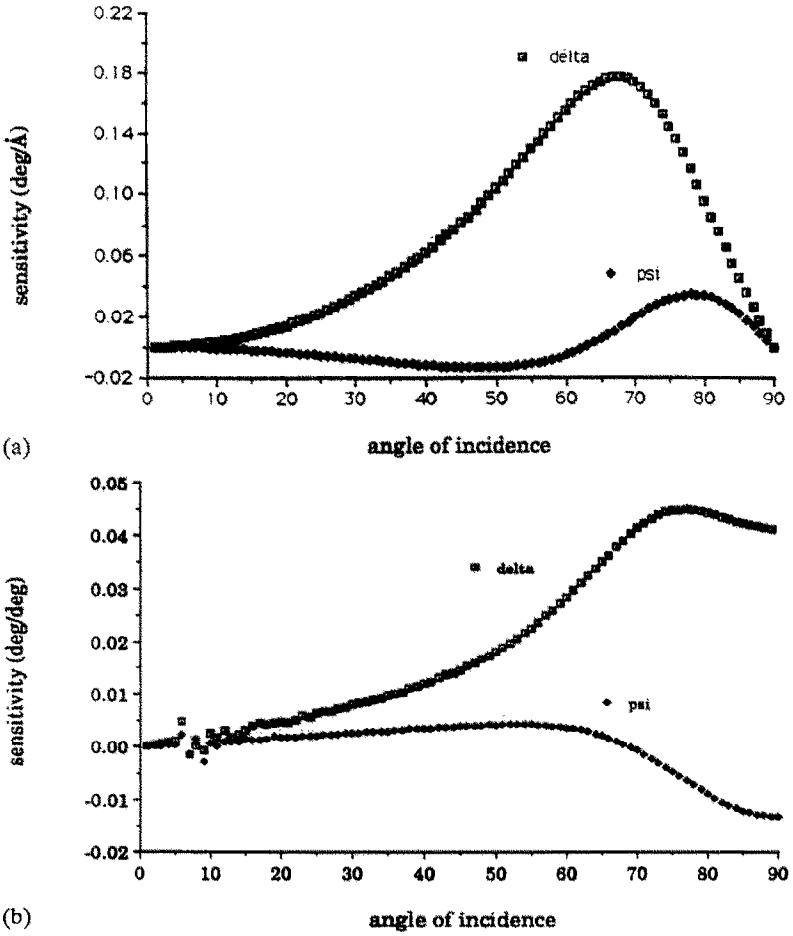

Fig. 3. Sensitivities of Δ (upper curves) and ψ (lower curves): (a) to an increase of 1 Å in the thickness of a 100 Å thick oxide film on a steel substrate, (b) to an error of 0.01° in the determination of the angle of incidence.

where Δ_i^m and ψ_i^m are measured and Δ_i^c and ψ_i^c are computed values at the ith of m angles of incidence. The components of vector $\boldsymbol{B}$ represent the fitted and fixed parameters which are n, k, d of film or films and n, k of the substrate. In the computations the fitted parameters of vector $\boldsymbol{B}$ are changed until a vector $\boldsymbol{B}_0$ is found such that the sum of the squares of the residuals G is minimum.

The success of this kind of iterative technique critically depends on the accuracy of the initial estimates for the solution [19]. To find the best initial estimates of parameters of an absorbing film on a substrate the following technique is used. Measurements at each angle of incidence give two equations. As described by McCrackin and Colson [20], several values of k are assumed, and the other unknowns n and d are calculated from the two equations for each value of k. These n and d values are plotted for a range of k values as in Fig. 4.

The sets of curves for n and d at different angles of incidence usually do not intersect at a single point owing to the systematic and random errors and to non-

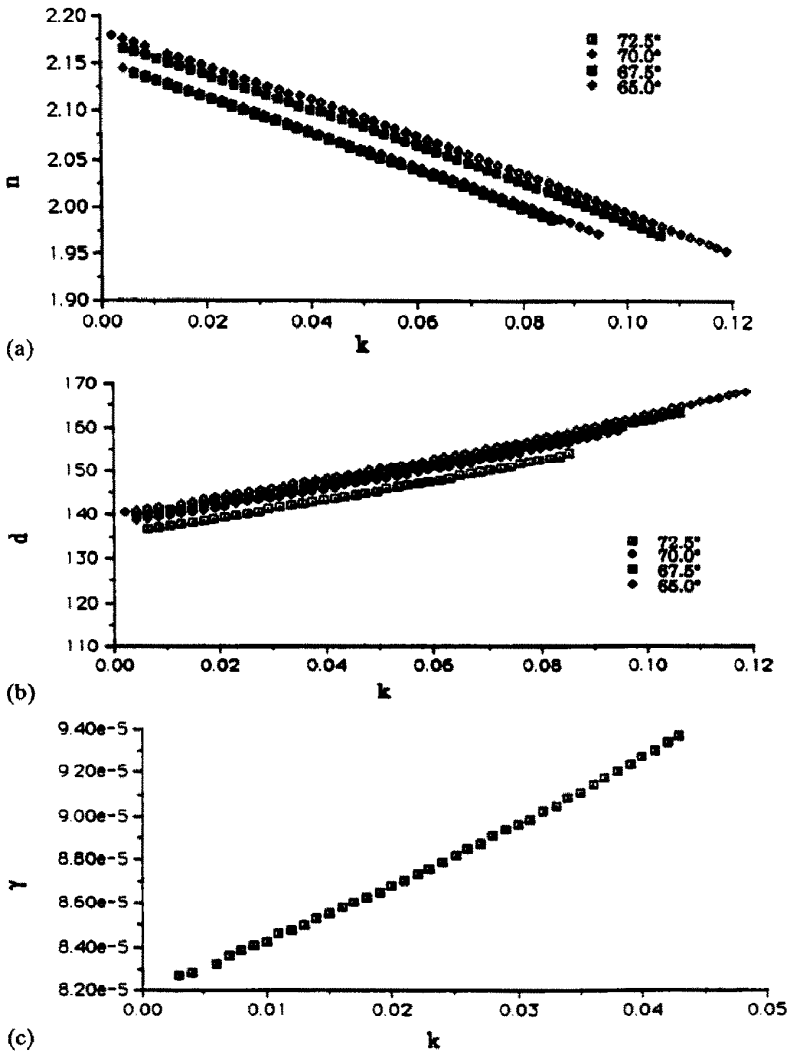

Fig. 4. (a) n *vs.* k solution curves for four angles between 65° and 72.5°, (b) d *vs.* k solution curves for four angles, (c) γ *vs.* k curve; minimum deviation γ_{min} occurred at $k=0.003$.

ideal effects of the substrate surface (*e.g.* roughness). Curves of n converge at high k values whereas curves of d converge at low k values. The errors and non-ideal effects shift the curves of different angles up or down rather than change their gradients significantly [21]. Therefore, the value of k which gives the minimum deviation among the n and d values for different angles is sought. The minimum deviation is defined as the minimum of the normalized multiplication product of the standard deviations of n and d values of different angles for a range of values of k.

For each assumed value of k the averages of n and d are computed:

$$n_{av}=\sum_{i=1}^{m} n_i s_i \qquad d_{av}=\sum_{i=1}^{m} d_i s_i \tag{30}$$

where m is the number of angles of incidence. Since the sensitivity of ellipsometry changes with the angle of incidence, the values of n and d at each angle of incidence must be weighted as proportional to Δ and ψ sensitivities at that angle. s_i is a weighting factor for each angle of incidence and is determined from Fig. 3(a).

Standard deviations of n and d around the average values are found by:

$$\sigma_n = \left\{ \sum_{i-1}^{m} (n_i - n_{av})^2 \right\}^{1/2} \qquad \sigma_d = \left\{ \sum_{i-1}^{m} (d_i - d_{av})^2 s_i \right\}^{1/2} \tag{31}$$

Since d, n and k are all coupled in the equations the deviation to be minimized must be the normalized product of σ_n times σ_d:

$$\gamma = \frac{\sigma_n \sigma_d}{n_{av} d_{av}} \tag{32}$$

After finding the value of k which gives the minimum deviation (γ_{min}), n_{av} and d_{av} at this value of k together with k are used in eqn. (29) as the initial estimates for the least squares fit, which in turn yields the solution set of fitted parameters which minimizes eqn. (29). In most of the cases minimum γ was obtained for very small values of k, between 0.001 and 0.05 as shown in Fig. 4(c).

8. Non-ideal effects of the ellipsometric measurements

As previously stated the Mueller matrix representation of the surfaces enables one to analyze the non-ideal effects. Every measured Mueller matrix for the specimens given in Figs. 7–9 in Part I [14] was analyzed for non-ideal effects using Williams' [11, 22] parameters: α, β, P_1, P_2, P_3, A_1, A_2, A_3. The parameter α was defined to quantify the degree of cross polarization. It is an angle whose value describes the extent to which an incident beam of light plane polarized either within or perpendicular to the plane of incidence contains components after reflection which are perpendicular to its original plane of polarization. Ideally, in the case of perfectly smooth specimen surfaces, α would be zero; an incident p- or s-wave would be reflected to produce a beam still polarized along the same direction. If reflection of such an incident beam resulted in light containing a component perpendicular to the original plane of polarization, then α would be non-zero. If such a reflection produced equal amounts of those two components, then α would be 90°.

The parameter β was defined to describe the change in ellipticity of the light which occurs upon reflection. Perfectly smooth surfaces should have no tendency to produce circularly polarized reflected light when the incident beam is either a p- or s-wave. Such ideal behavior corresponds to a value of β equal to zero. If an incident p- or s-wave were reflected as right-handed circularly polarized light, then β would be +90°. Qualitatively, β can be regarded as measure of the right- or left-handedness of the surface.

Polarization parameters, P_1, P_2 and P_3, describe the extent to which the reflected light is depolarized. They are defined respectively as the fractions of the reflected light which remain polarized when the incident light is plane polarized at angles of either 0° or 90° (P_1) (the p- or s-wave), plane polarized at angles of +45° or −45° relative to the plane of incidence (P_2), and right or left circularly polarized (P_3). If the specimen surface were perfectly smooth, then all three parameters would be unity. If the reflected light were totally depolarized, they would all be zero. A_1, A_2, and A_3

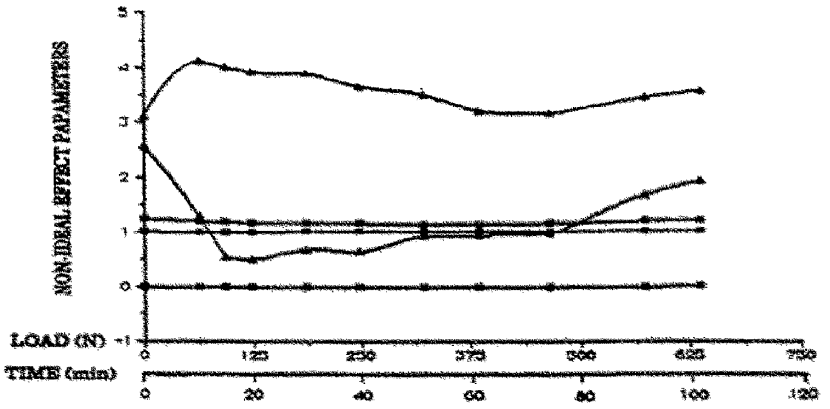

(a)

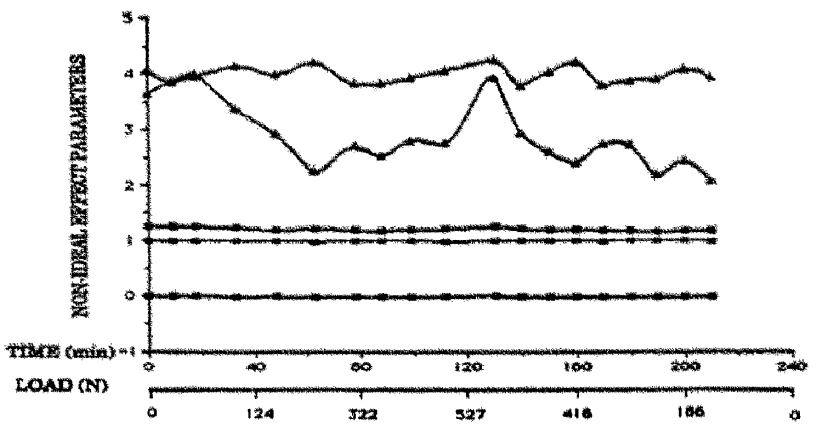

(b)

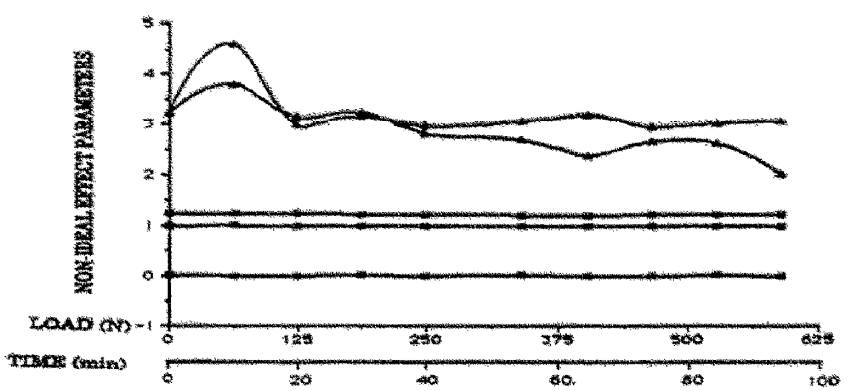

(c)

Fig. 5. Non-ideal effect parameters: (a) 45-M specimen, (b) 54-M specimen, (c) 60-M specimen. Top curve β; second curve α; third curve, P_2, P_3; fourth curve P_1; bottom curve A_1, A_2, A_3.

represent asymmetry in the amounts of depolarization of the oppositely directed input vectors. These parameters follow the Stokes convention for the designation of polarization state of light. A more thorough definition of these parameters is given in ref. 11 and their practical applications on rough surfaces are given in ref. 22.

In ref. 22 it was shown that the surface roughness effects are most pronounced at 70° angle of incidence. When Δ and ψ parameters are changed significantly owing to surface roughness effects, the non-ideal effect parameters are changed significantly too. In this way, the effect of surface irregularities on Δ and ψ parameters can be judged from the change in non-ideal effect parameters during sliding. The changes in non-ideal effect parameters are given in Figs. 5(a), (b) and (c) for 45, 54 and 60 HRC specimens respectively for the 70° angle of incidence. P and A parameters were very close to the ideal values and did not change throughout the experiments. At the beginning of sliding, α and β were a few degrees off from their ideal value which is zero. Small changes in α and β were observed throughout the experiments; however, in most cases the changes were towards the ideal. Therefore, we can conclude that non-ideal effects on the ellipsometric data due to changes in surface roughness during sliding experiments were minimal and did not interfere much with the calculation of film parameters.

The Ohlidal–Lukes theory [21] predicts that the effect of surface roughness on Δ and ψ is comparable with random errors for root mean square slopes of asperities up to 0.01. For a root mean square slope of 0.04 the errors in optical constants determined by ellipsometry due to neglecting the roughness of the surface is less than 1% (ref. 21). In our case, final root mean square slopes across the sliding track were 0.039, 0.19 and 0.011 for 45, 54 and 60 HRC specimens respectively. Along the sliding track the root mean square slopes were less than 0.01 for all three specimens. This means that the effect of surface roughness, theoretically, produces less than 1% error in our data analysis.

Acknowledgment

We are grateful to the National Science Foundation and in the person of Dr. J. Larsen-basse for financial support.

References

1 S. C. Kang and K. C. Ludema, The breaking-in of lubricated surfaces, *Wear, 108* (1986) 375–384.
2 M. Suzuki and K. C. Ludema, The wear process during the running-in of steel in lubricated sliding, *ASME paper, 86-Trib-44,* AMSE, New York, 1986.
3 M. W. Williams, Ellipsometric evidence for the formation of Fe_3O_4 during unlubricated sliding of 4340 steel, in K. C. Ludema (ed.), *Proc. Conf. on Wear of Materials, Houston, TX, 1987,* Vol. 1, 1987, pp. 219–222.
4 I. Ohlidal, K. Navratil and F. Lukes, Reflection of light by a system of nonabsorbing isotropic film–nonabsorbing isotropic substrate with randomly rough boundaries, *J. Opt. Soc. Am., 61* (12) (1971) 1630–1639.
5 I. Ohlidal and F. Lukes, Ellipsometric parameters of rough surfaces and of a system substrate–thin film with rough boundaries, *Opt. Acta, 19* (10) (1972) 817–843.
6 T. V. Vorburger and K. C. Ludema, Ellipsometry of rough surfaces, *Appl. Opt., 19* (1980) 561–573.
7 Y. Fainman, J. Shamir, D. Peri and A. Brunfeld, Polarization properties of speckle patterns scattered from rough conductors, *J. Opt. Soc. Am. A, 4* (12) (1987) 2205–2212.

8 C. A. Fenstermaker and F. L. McCrackin, Errors arising from surface roughness in ellipsometric measurement of the refractive index of a surface, *Surf. Sci, 16* (1969) 85–96.
9 D. E. Aspnes, J. B. Theeten and F. Hottier, Investigation of effective-medium models of microscopic surface roughness by spectroscopic ellipsometry, *Phys. Rev. B, 20* (1979) 3292–3302.
10 D. A. Ramsey, Mueller matrix ellipsometry involving extremely rough surfaces, *Ph.D. Thesis,* University of Michigan, Ann Arbor, MI, 1985.
11 M. W. Williams, Depolarization and cross polarization in ellipsometry of rough surfaces, *Appl. Opt., 25* (20) (1986) 3616–3622.
12 W. A. Shurcliff, *Polarized Light,* Harvard University Press, Cambridge, MA, 1962.
13 P. S. Hauge, Mueller matrix ellipsometry with imperfect compensators, *J. Opt. Soc. Am., 68* (11) (1978) 1519–1528.
14 B. Çavdar and K. C. Ludema, Dynamics of dual film formation in boundary lubrication of steels. Part I: functional nature and mechanical properties, *Wear, 148* (1991) 303.
15 O. S. Heavens, *Optical Properties of Thin Solid Films,* Dower, New York, 1965.
16 R. C. Smith and M. Hacskaylo, Factors influencing the experimental sensitivity of the Drude technique, *Ellipsometry in the Measurements of Surfaces and Thin Films Symp. Proc., Washington, 1963,* N.B.S. Misc. Pub. 256, pp. 83–95.
17 R. M. A. Azzam and N. M. Bashara, *Ellipsometry and Polarized Light,* North-Holland, Amsterdam, 1977, pp. 305–312.
18 D. W. Marquardt, An algorithm for least-squares estimation of nonlinear parameters, *J. Soc. Ind. Appl. Math, 11* (1963) 431–441.
19 D. G. Shueler, Error analysis of angle of incidence measurements, *Surf. Sci., 16* (1969) 104–111.
20 F. L. McCrackin and J. P. Colson, Computational techniques for the use of the exact Drude equations in reflection problems, *Ellipsometry in the Measurements of Surfaces and Thin Films Symp. Proc., Washington, 1963,* N.B.S. Misc. Pub. 256, pp. 60–82.
21 I. Ohlidal, F. Lukes and K. Navratil, Rough silicon surfaces studied by optical methods, *Surf. Sci., 45* (1974) 91–116.
22 M. W. Williams, K. C. Ludema and D. M. Hildreth, Mueller matrix ellipsometry of practical surfaces, *Surf. Topography, 1* (1988) 111–126.